Integrated Geophysical Studies on the Basement Structure of the Arkoma Basin, Oklahoma and Arkansas*

Hamed Alrefaee[1], G. Randy Keller[1], and Kurt J. Marfurt[1]

Search and Discovery Article #50710 (2012)**
Posted August 31, 2012

*Adapted from oral presentation at AAPG Annual Convention and Exhibition, Long Beach, California, April 22-25, 2012

[1]University of Oklahoma, Norman, OK (hamrefaee@ou.edu)

Abstract

The Arkoma Basin is an arcuate structural feature that extends from the Gulf coastal plain in central Arkansas westward 400 km to the Arbuckle Mountains in south-central Oklahoma. The basin is characterized by down-to-the-south normal faults that affect Early Pennsylvanian and older rocks. Many folds in the Arkoma basin were produced by horizontal compressive forces related to the Ouachita orogeny. The compressive forces were directed north and northwest and decreased in intensity away from the Ouachita Mountains region. However, the deep structure of the basin is poorly known, and Precambrian basement structures in other areas of the continental United States have strongly influenced later Proterozoic and Phanerozoic tectonism within the continent.

The aim of this paper is to map the basement surface and the associated structural elements in the Arkoma basin area as well as to investigate the relationship between these structures and the Phanerozoic tectonic deformation in the area. We are calculating the depth to the basement surface using the Euler magnetic depth estimation method. Structural interpretation of the 3D seismic data of the basement surface is being conducted. Coherence and curvatures as well as other seismic attributes will be applied to the 3D seismic volume to delineate different subtle structural and stratigraphic features affecting the basement surface. Gravity modeling is being used as the integrative platform to synthesize seismic and well data and the depths obtained using the Euler technique.

References

Arbenz, J.K., 2008, Structural framework of the Ouachita Mountains, *in* N.H. Suneson, (ed.), Stratigraphy and structural evolution of the Ouachita Mountains and Arkoma Basin, southeastern Oklahoma and west-central Arkansas, applications to petroleum exploration; 2004 field symposium: Oklahoma Geological Survey Circular, Report # 112A, p. 1-40.

Barnes, C.G., W.M. Shannon, and H. Kargi, 1999, Diverse Mesoproterozoic basaltic magmatism in West Texas, *in* C.D. Frost, (ed.), Proterozoic magmatism of the Rocky Mountains and environs (Part 1): Rocky Mountain Geology, v. 34/2, p. 263-273.

Elebiju, O.O., G.R. Keller, and K.J. Marfurt, 2008, New structural mapping of basement features in the Fort Worth basin, Texas, using high-resolution aeromagnetic derivatives and Euler depth estimates: Earth Scientist, The University of Oklahoma, ConocoPhillips School of Geology and Geophysics, p. 46 – 48.

Houseknect, D.W., and S.M. Matthews, 1985, Thermal maturity of the carboniferous strata, Ouachita Mountains: AAPG Bulletin, 69/3, p. 335-345.

Keller, G.R., E.G. Lidiak, W.J. Hinze, and L.W. Braile, 1983, The role of rifting in the tectonic development of the midcontinent, USA: Tectonophysics, v. 94, p. 391-412.

Keller, G.R., K. Karlstom, and G.L. Farmer, 1999, Tectonic evolution in the Rocky Mountain region: 4-D imaging of the continental lithosphere: EOS, Transactions of the American Geophysical Union, v. 80, p. 493, 495, 498. (or show it 493-498?)

Keller, G.R., L.W. Braile, G.A. McMechan, W.A. Thomas, S.H. Harder, W. Chang, and W.G. Jardine, 1989, The Paleozoic continent-ocean transition in the Ouachita Mountains imaged from PASSCAL wide-angle seismic reflection-refraction data: Geology, v. 17, p. 119-122.

Keller, G.R., and R.D. Hatcher, Jr., 1999, Comparison of the lithospheric structure of the Appalachian – Ouachita orogeny and Paleozoic orogenic belts in Europe: Tectonophysics, v. 314, p. 43-68.

Phillips, J.D., M.N. Nabighian, D.V. Smith, and Y. Li, 2007, Estimating locations and total magnetization vectors of compact magnetic sources from scalar, vector, or tensor magnetic measurements through combined Helbig and Euler analysis: SEG 77th Annual Meeting, San Antonio, Texas, 5 p.

Reid, A.B., J.M. Allsop, H. Granser, A.J. Millett, and I.W. Somerton, 1990, Magnetic interpretation in three dimensions using Euler deconvolution: Geophysics, v. 55/1, p. 80-91.

Smith, G.J., and R.D. Jacobi, 2005, The influence of basement structures on Upper Devonian deposition in New York State: AAPG Search and Discovery Article # 90039. Web accessed 21 August 2012.
http://www.searchanddiscovery.com/abstracts/html/2005/annual/abstracts/smith03.htm

Thompson, D.T., 1982, EUKDPH – a new technique for making computer-assisted depth estimates from magnetic data: Geophysics, v. 47, p. 31-37.

Van Schmus, W.R., M.E. Bickford, and A. Turek, 1996, Proterozoic geology of the east-central Midcontinent basement, *in* B.A. van der Pluijm, and P.A. Catacosinos, (eds.), Basement and basins of Eastern North America: GSA Special Paper 308, p. 7-32.

Verduzco, B., J.D. Fairhead, C.M. Green, and C. MacKenzie, 2004, New insights into magnetic derivatives for structural mapping: Leading Edge, v. 23/2, p. 1161-119.

Viele, G.W., and W.A. Thomas, 1989, Tectonic synthesis of the Ouachita orogenic belt, *in* R.D. Hatcher, Jr., W.A. Thomas, and G.W. Viele, (eds.), The Appalachian-Ouachita orogeny in the United States: GSA, The Geology of North America, v. F-2, p. 695-728.

ConocoPhillips SCHOOL OF GEOLOGY & GEOPHYSICS
The University of Oklahoma

Integrated Geophysical Studies on the Basement Structure of the Arkoma Basin, Oklahoma and Arkansas

Hamed Alrefaee

G. Randy Keller & Kurt J. Marfurt

Outlines

- Aim of study
- Tectonic background
- Regional geology and structural setting
- Study area
- Methodology
  - *Gravity and magnetic data analysis*
  - *Seismic data analysis*
  - *Well data*
- Conclusion

Aim of the study

The study aims to integrate 3D seismic, gravity and magnetic data as well as well data for better mapping and illumination of the basement structures in Arkoma basin.

Importance of mapping basement structures:

- ***Precambrian basement structures have strongly affected the Phanerozoic tectonics in the continental United States (Smith et. al., 2005).***
- ***Basement structures in Fort Worth Basin are responsible for the intra-sedimentary features such as faults, fractures and collapse features in the Ellenberger Group and Viola Limestone, (Elebiju et. al., 2008)***

Tectonic Background

- **The North America continent**
  1- Plate collision of Archean and Proterozoic blocks
  2- Progressive addition of volcanic arcs and oceanic terranes accreted along southern plate margins.

- **Rodinia, a supercontinent, was the result of continental growth.**

- **Rodinia began to break up apart around 600 Ma.**

- **Rifted margin developed about 550 Ma (Keller et. al., 1983). Passive continental margin with carbonate deposition.**

- **The southern margin changed to active margin characterized by clastic sedimentation (Viele and Thomas, 1989).**

- **Subduction and collision developed**

- **The Ouachita orogenic belt developed as the result of the collision and Arkoma basin was formed as a foreland basin.**

Regional Geology and Tectonic Setting

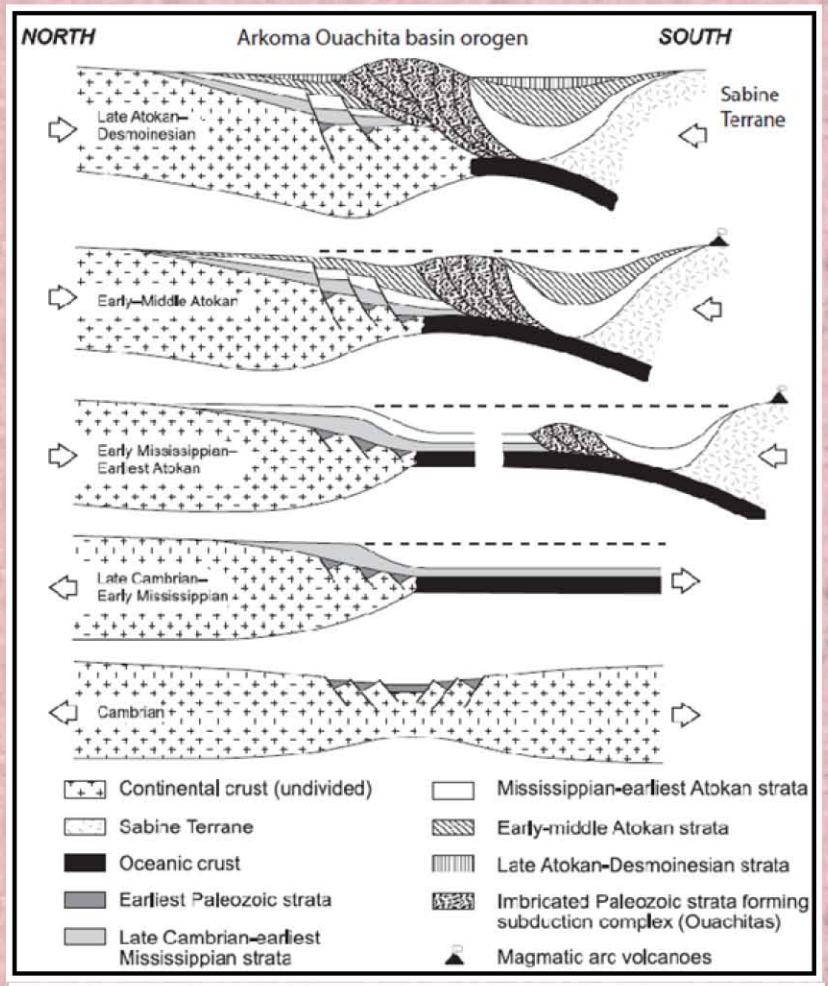

Tectonic evolution of Arkoma basin and Ouachita orogenic belt, Houseknect and Matthews (1985).

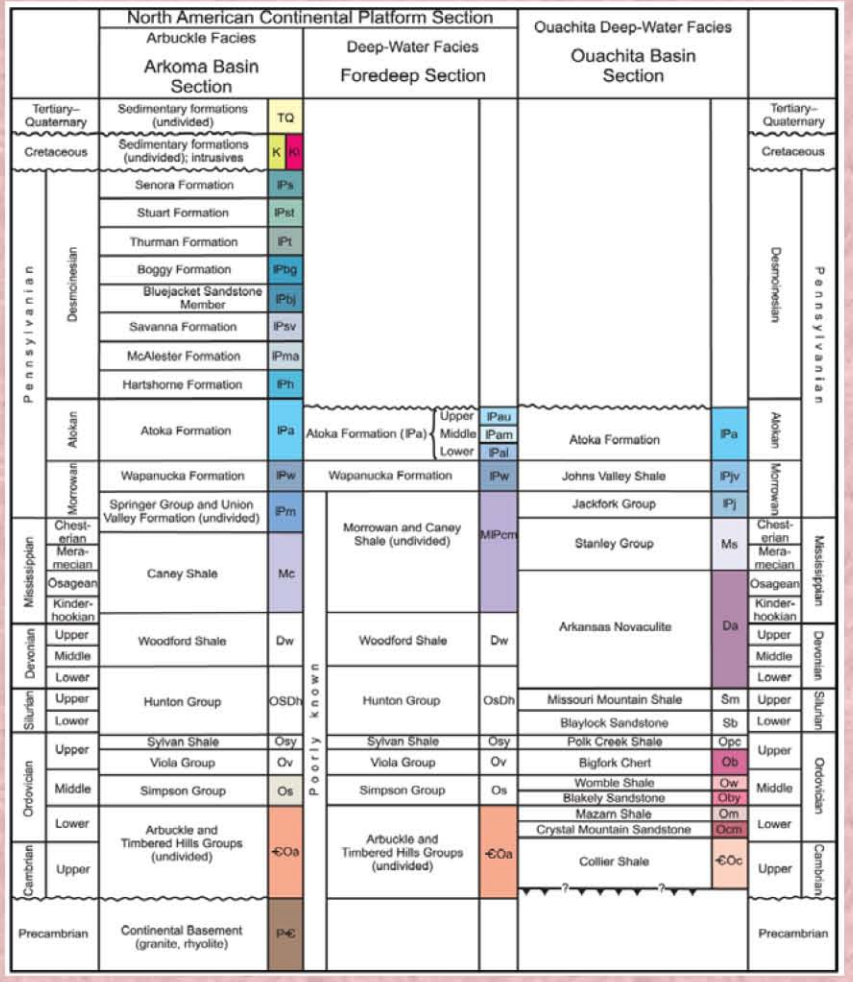

Stratigraphic section of Arkoma basin, Arbenz 2008.

Location map of study area

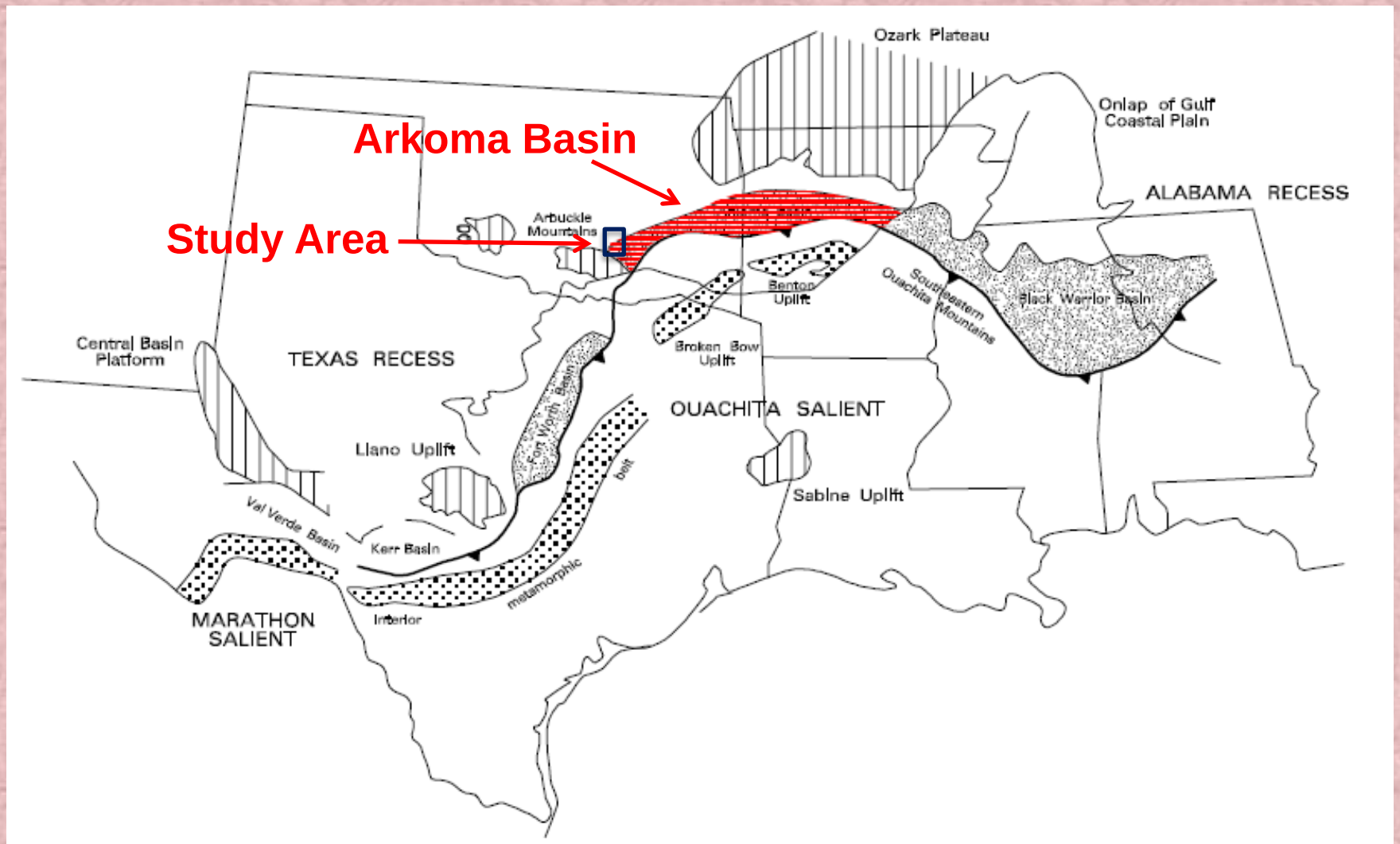

Structural Cross Section

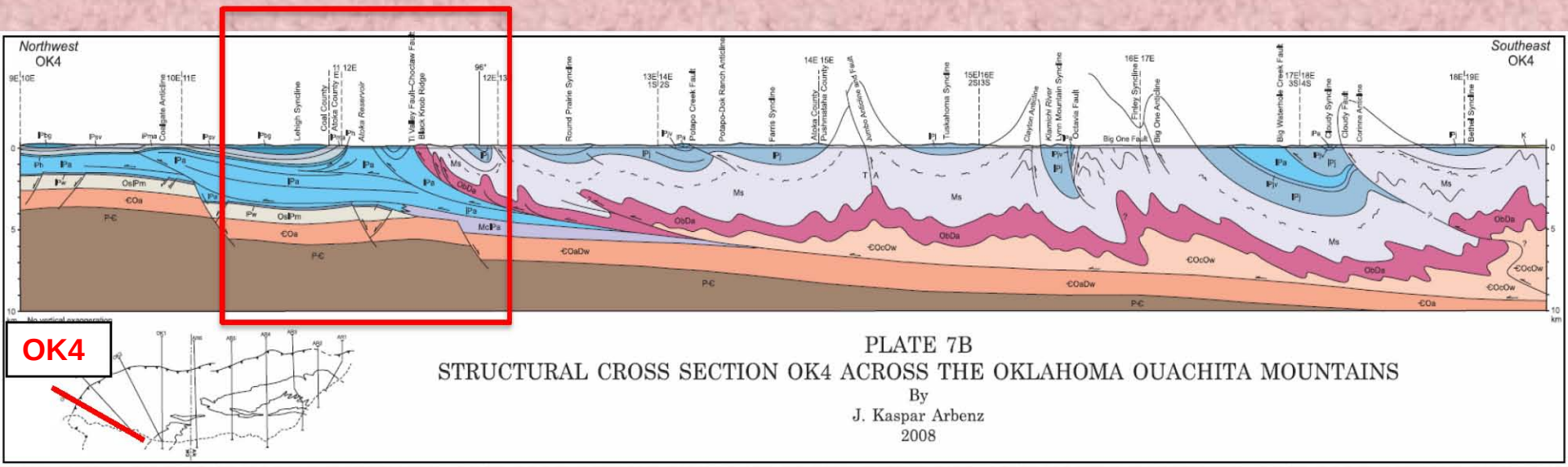

PLATE 7B

STRUCTURAL CROSS SECTION OK4 ACROSS THE OKLAHOMA OUACHITA MOUNTAINS

By

J. Kaspar Arbenz

2008

Structural cross section OK4 along Ouachita orogenic belt, Arbenz, 2008.

Structural Setting of the Study Area

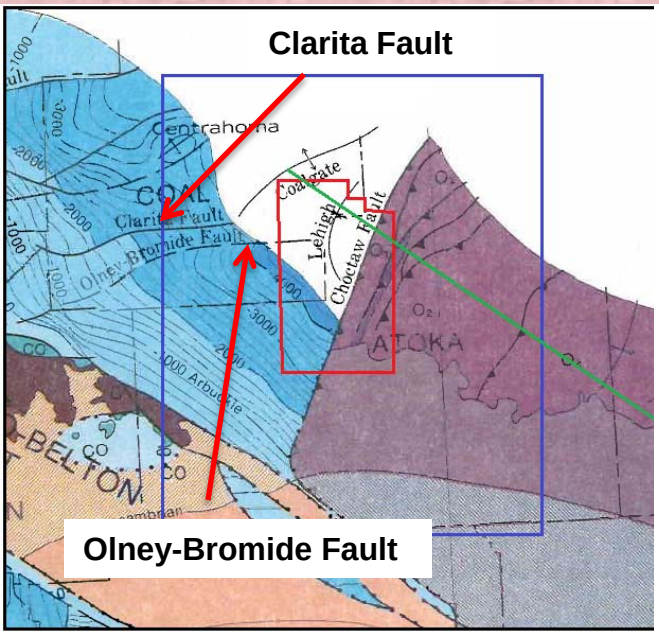

Location map of the study area shows the seismic survey outlines in red, Euler magnetic depth estimation in black and structural cross section profile in green colors.

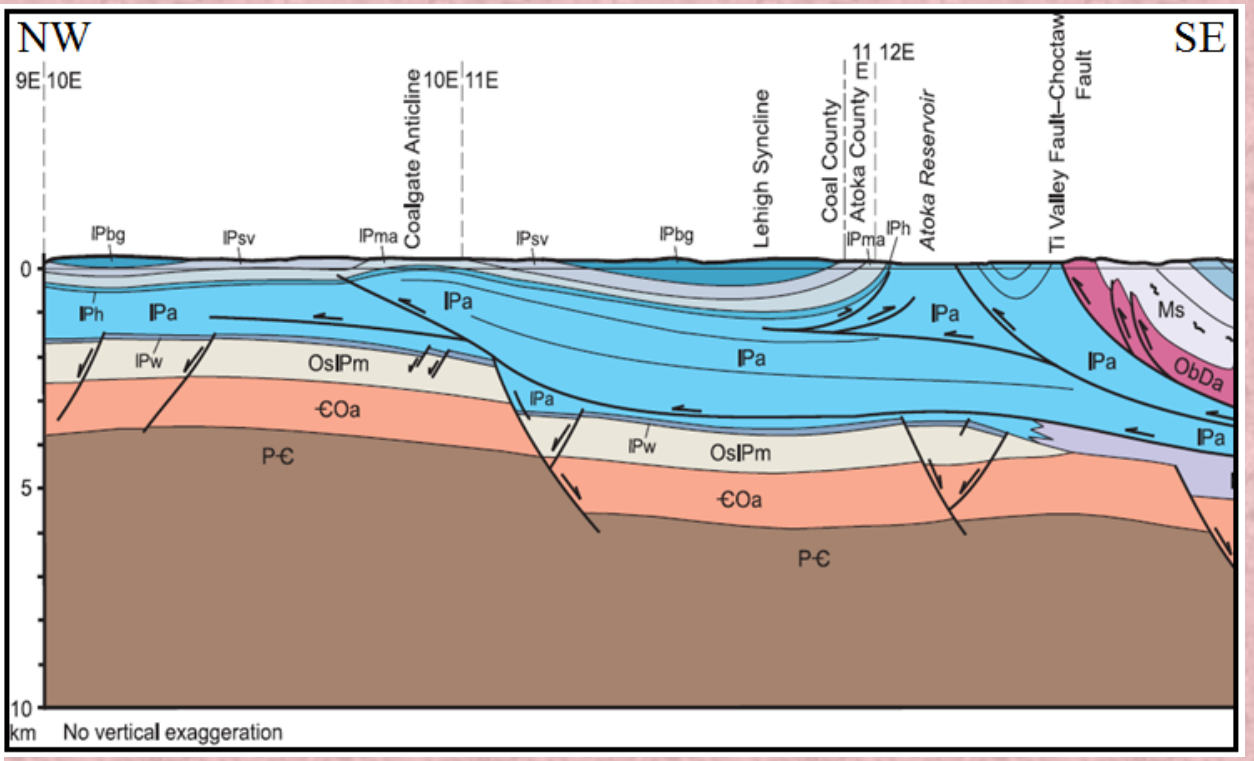

Structural cross section along the green profile Arbenz, 2008.

Methodology

- **Magnetic data**
  - *Edge Detection Techniques*
  - *Euler Depth Estimation Method*
- **3D seismic data**
  - *Interpretation of the faults*
  - *Volumetric seismic attributes (enhances the faults appearance)*
  - *Picking the basement surface*
  - *Seismic surface attributes through the basement surface*
- **Gravity and well data**
  - *Separation of residual-regional anomaly*
  - *Density models along selected profiles on the residual gravity map*
  - *Top to the Arbuckle & top to the basement*
  - *Densities for the formations (Regional models and literature)*

Gravity and Magnetic Data Analysis

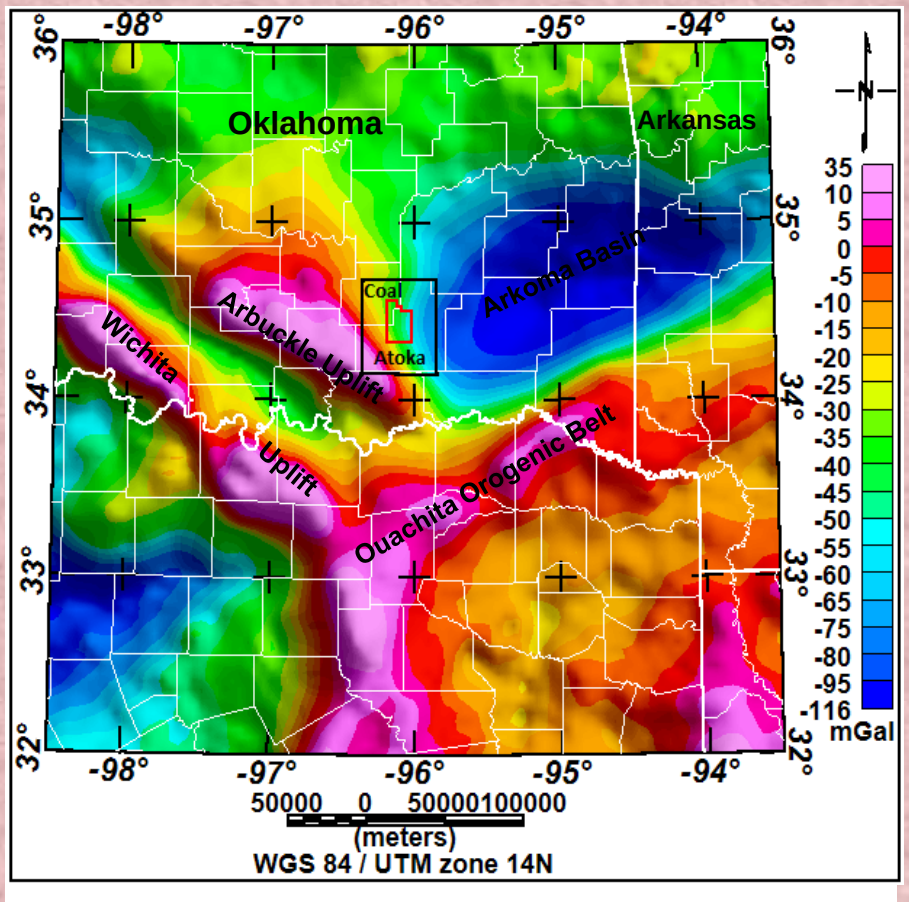

Bouguer gravity map of Arkoma basin and its surrounding. The seismic survey outlines is shown in red, Euler magnetic depth estimation in black.

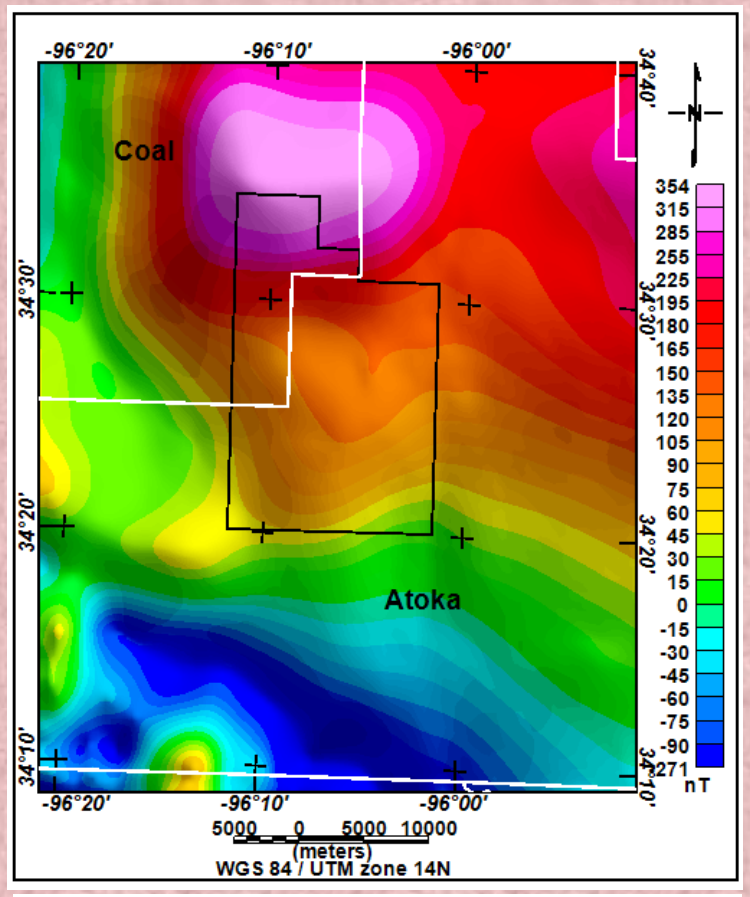

Total magnetic intensity map of the area shown by black rectangle.

Gravity and Magnetic Data Analysis

Edge Detection Techniques

The total horizontal derivative peaks over the edges and is zero over the body.

Total horizontal derivative

$$THD = \sqrt{\left(\frac{dT}{dX}\right)^2 + \left(\frac{dT}{dY}\right)^2}$$

Where T is the magnetic or gravity field

(Verduzco et. al., 2004)

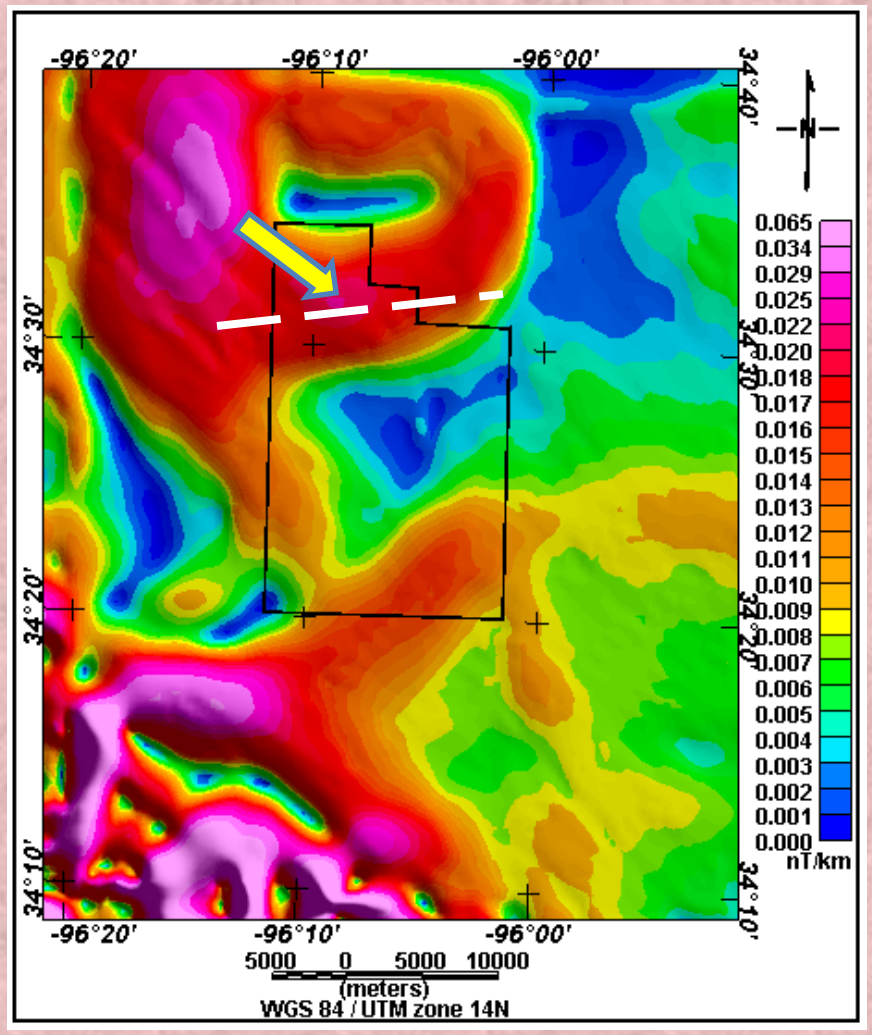

Total Horizontal Derivative of magnetic data

Gravity and Magnetic Data Analysis

Edge Detection Techniques

The tilt derivative has high positive value over the source and low value (close to zero) at/or near the edge.

Tilt Derivative

$$TD = \tan^{-1}\left(\frac{VD}{THD}\right)$$

VD *vertical component of* gradient

THD horizontal component of gradient

(Verduzco et. al., 2004)

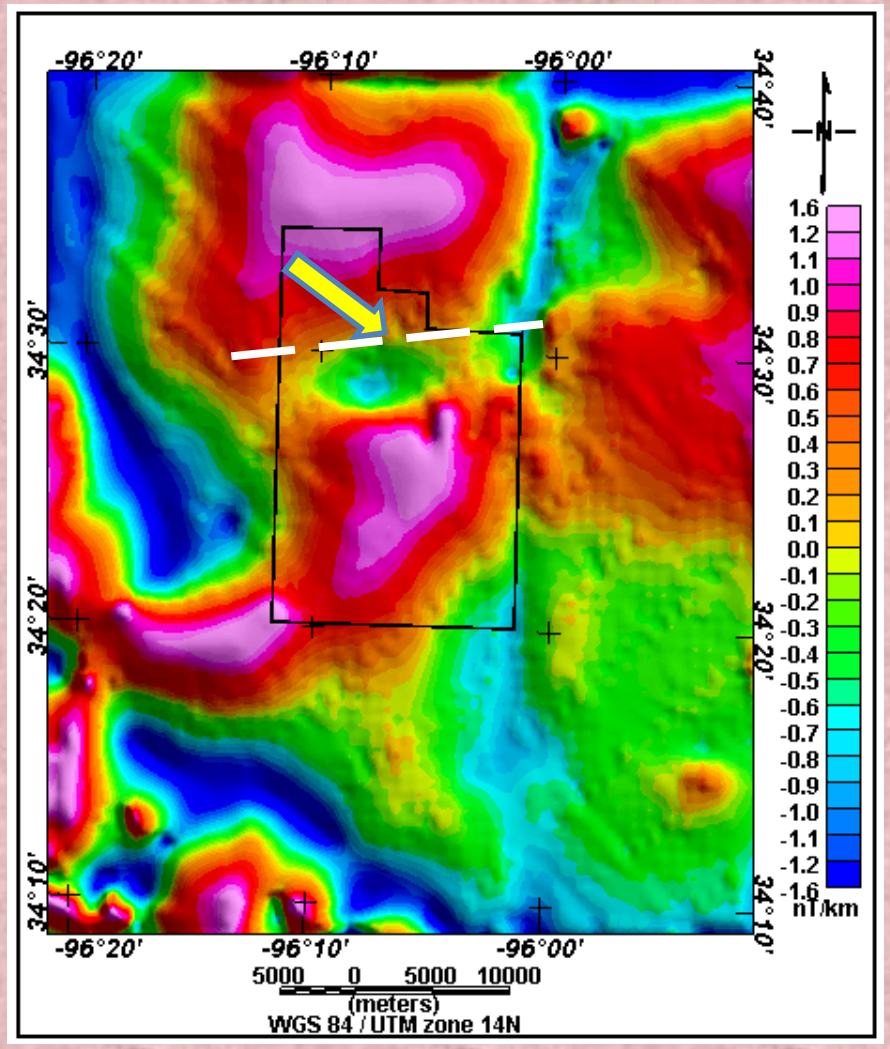

Tilt Derivative of magnetic data

Gravity and Magnetic Data Analysis

Basement Depth Estimation
Euler Deconvolution Method

- **Determine the location and depth to magnetic source (Phillips, 2007).**
- **Delineate magnetic boundary or fault trends (Reid et al., 1990).**

Euler's homogeneity relation

$$(x-x_0)\frac{\partial T}{\partial x}+(y-y_0)\frac{\partial T}{\partial y}+(z-z_0)\frac{\partial T}{\partial z}=N(B-T)$$

where (x_0, y_0, z_0) is the position of a source, whose total field *T* is detected at (*x*, *y*, *z*).

***B* is the regional field or background value.**

***N* is the degree of homogeneity, and geophysicaly known as a structural index (SI: Thompson, 1982).**

Gravity and Magnetic Data Analysis

Euler Depth Estimation Method Results

Euler solution plot using structural index (SI=0.0 faults) shows clustering of magnetic sources solutions along some trends which may reflect fault directions. The maximum depth to these faults is about 3500 meters.

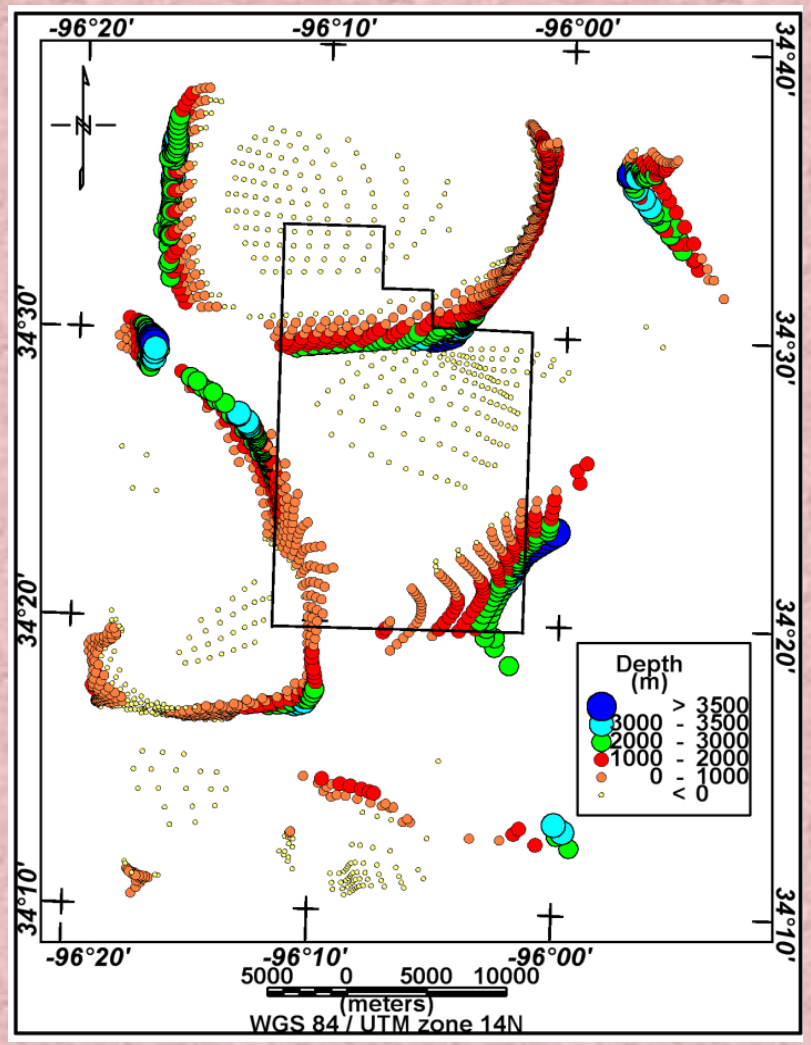

Gravity and Magnetic Data Analysis

Euler Depth Estimation & Edge Detection

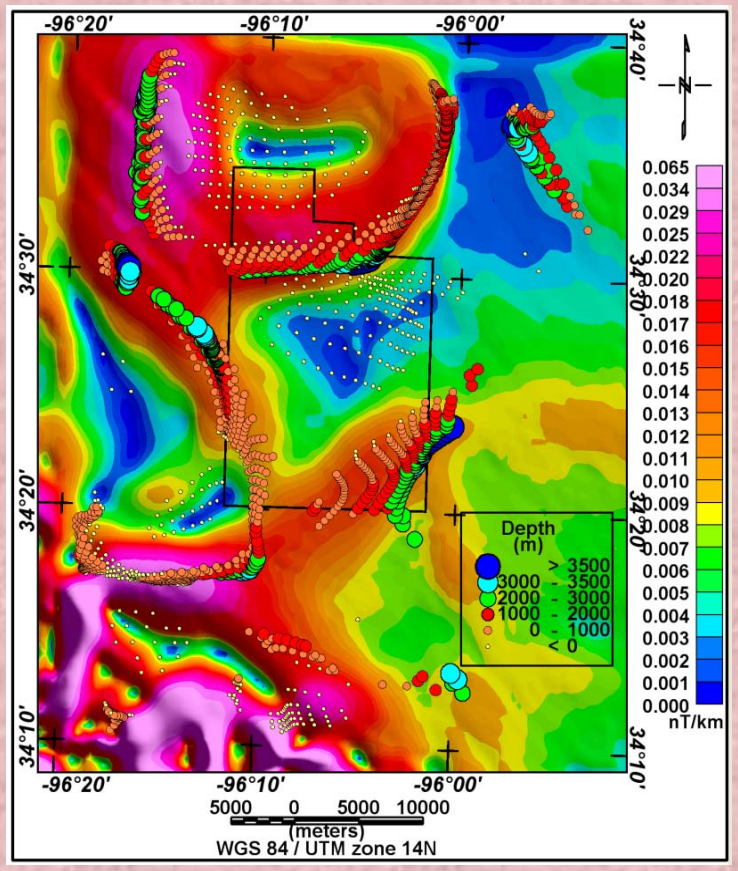

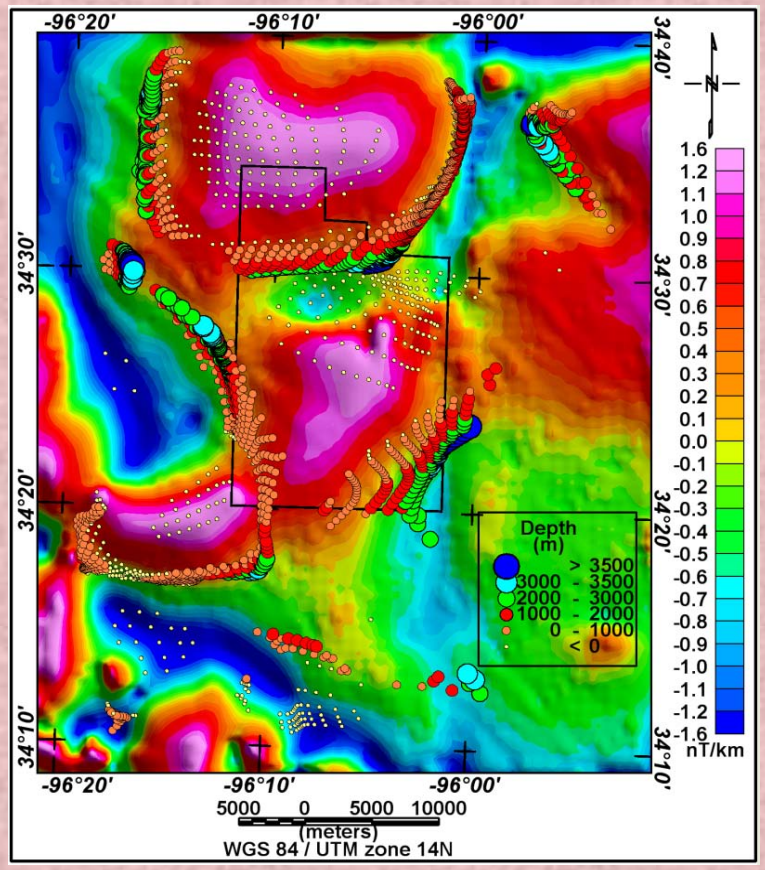

Two figures show the solution cluster superimposed on the total horizontal derivative and tilt derivative of the magnetic data. The cluster shows good correlation with the edges of the source body.

3D Seismic Data and Seismic Attributes

Interpretation of Basement Structures

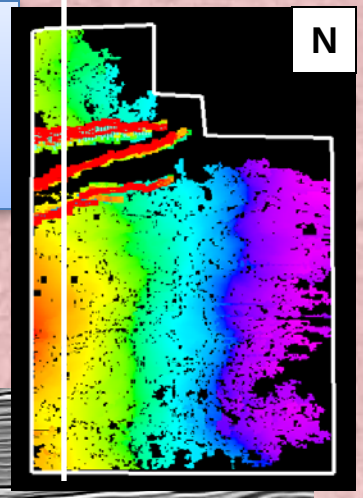

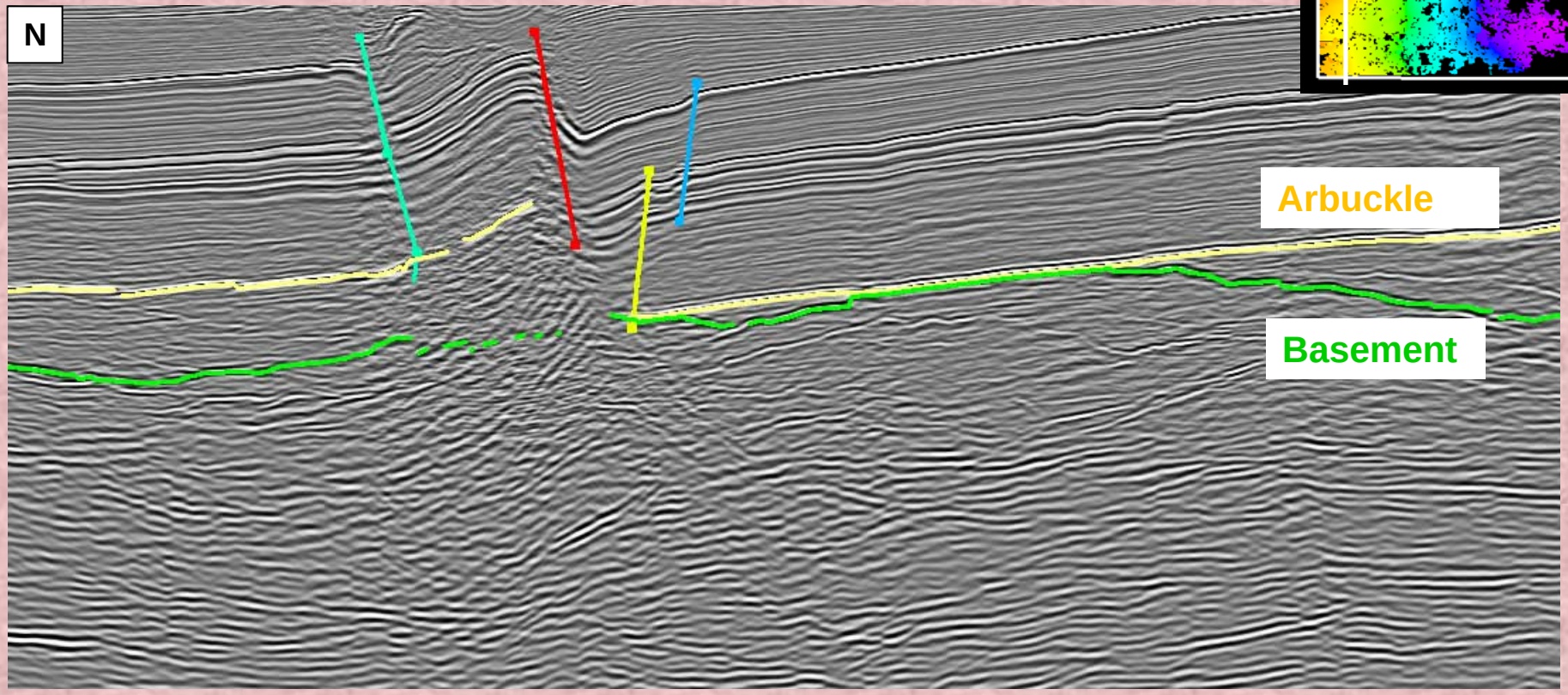

Vertical slice (Xline 180) with initial interpretation of some faults, basement, and Arbuckle horizons.

3D Seismic Data and Seismic Attributes

Volumetric Attributes (Coherence)

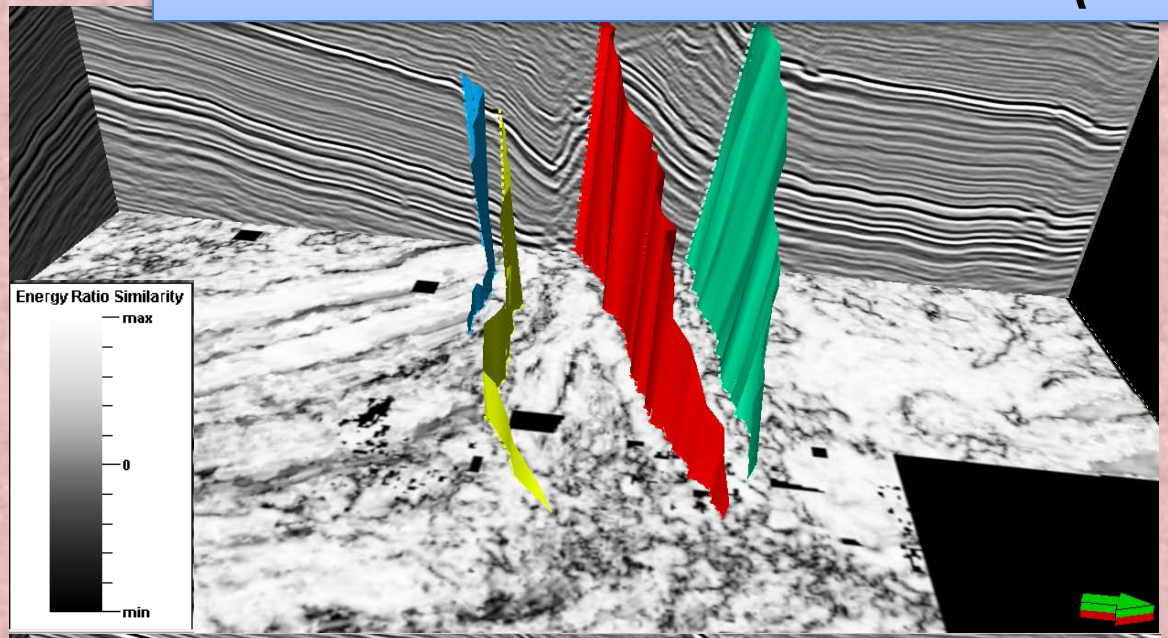

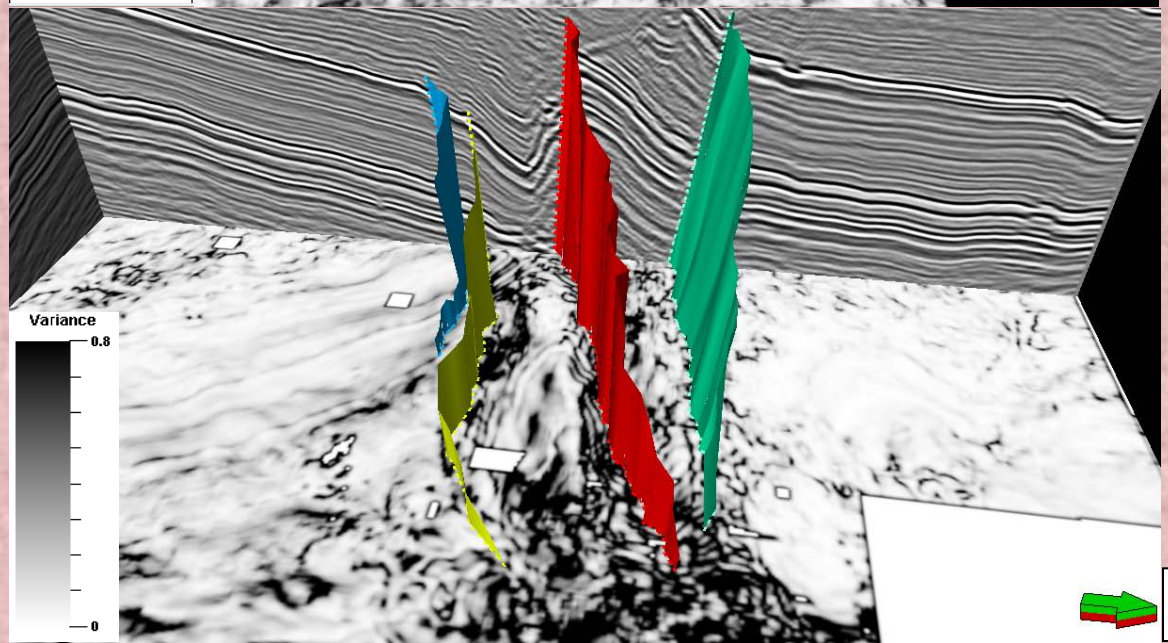

Time slices (1650 ms) through the coherence and variance volumes show the discontinuities (faults and deformed zones) as incoherent black lineaments.

3D Seismic Data and Seismic Attributes

Volumetric Attributes (Curvature)

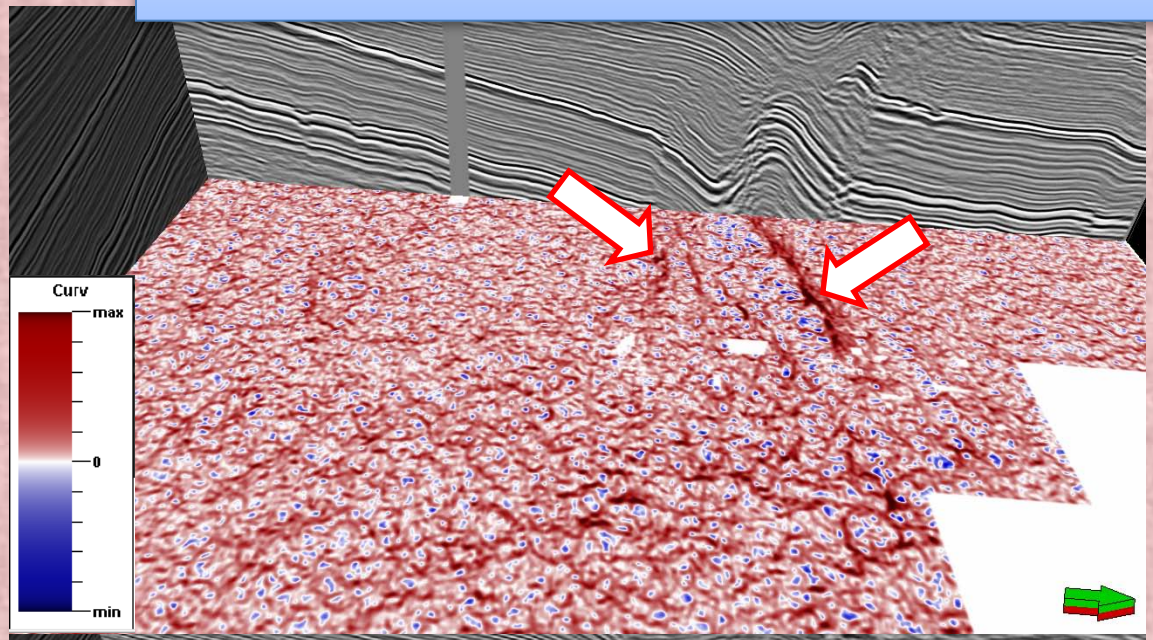

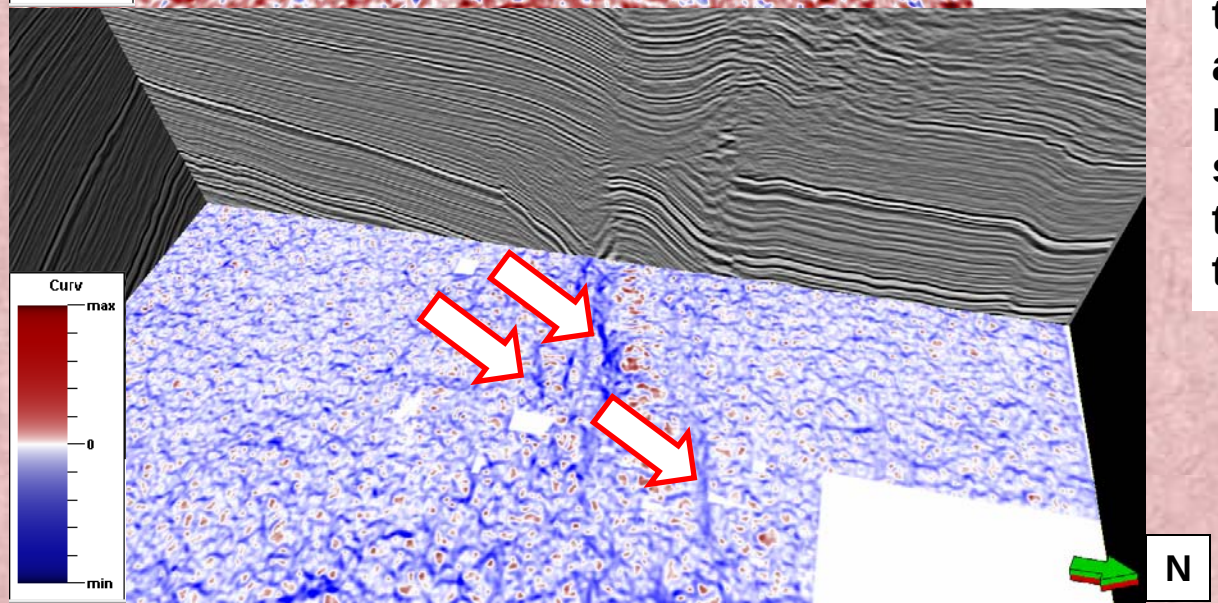

Time slices (1500 ms) through the most positive and most negative curvatures volumes shows the faults trends.

The most positive curvature shows maximum values over the upthrown blocks and the anticlinal features, while the most negative curvature shows maximum values over the downthrown blocks and the synclinal features.

3D Seismic Data and Seismic Attributes

Generating the basement surface

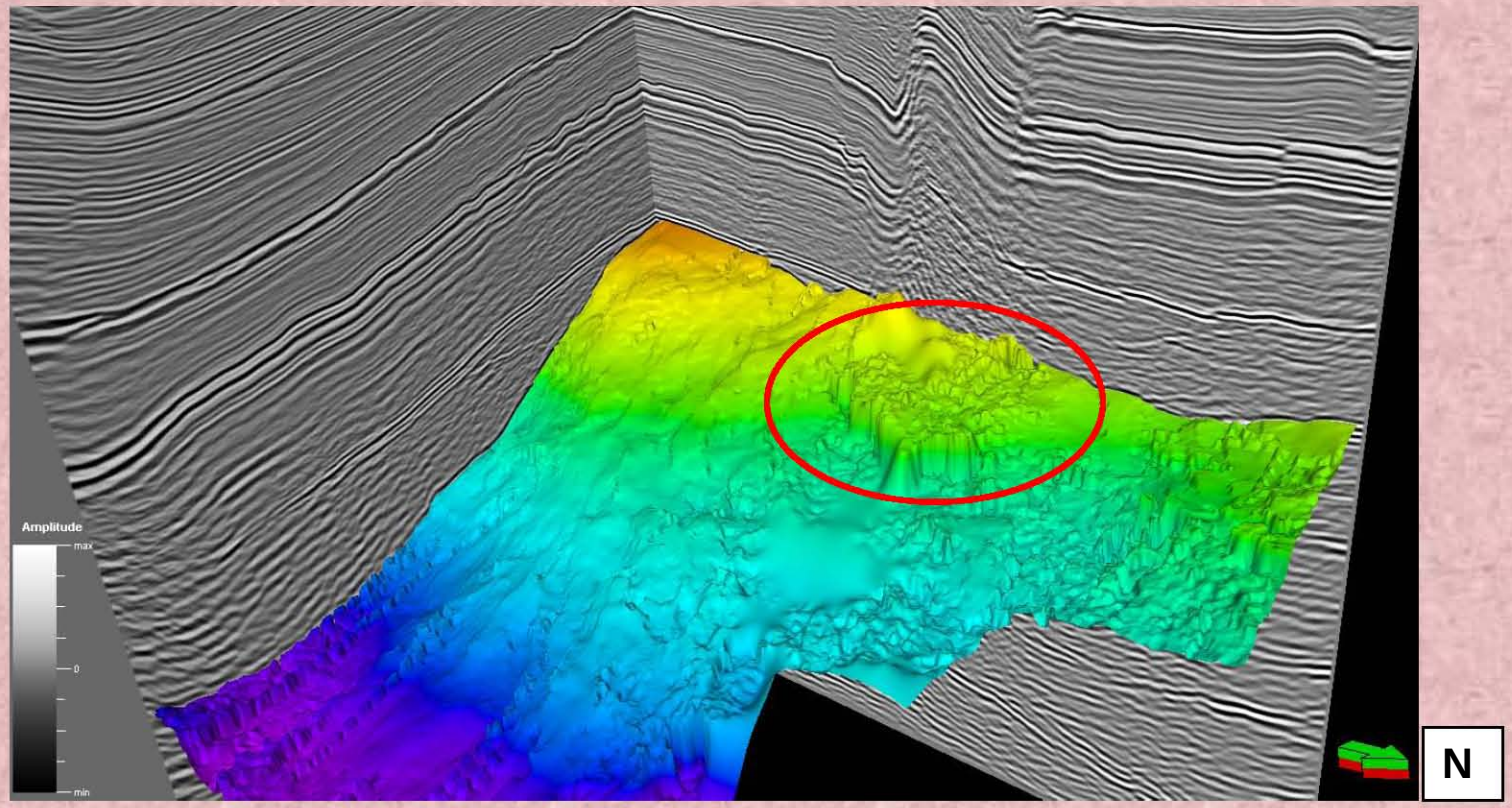

3D view shows the basement surface with intensive irregular topography due to erosion and an area of extensive deformation.

3D Seismic Data and Seismic Attributes

Seismic attributes through the basement surface

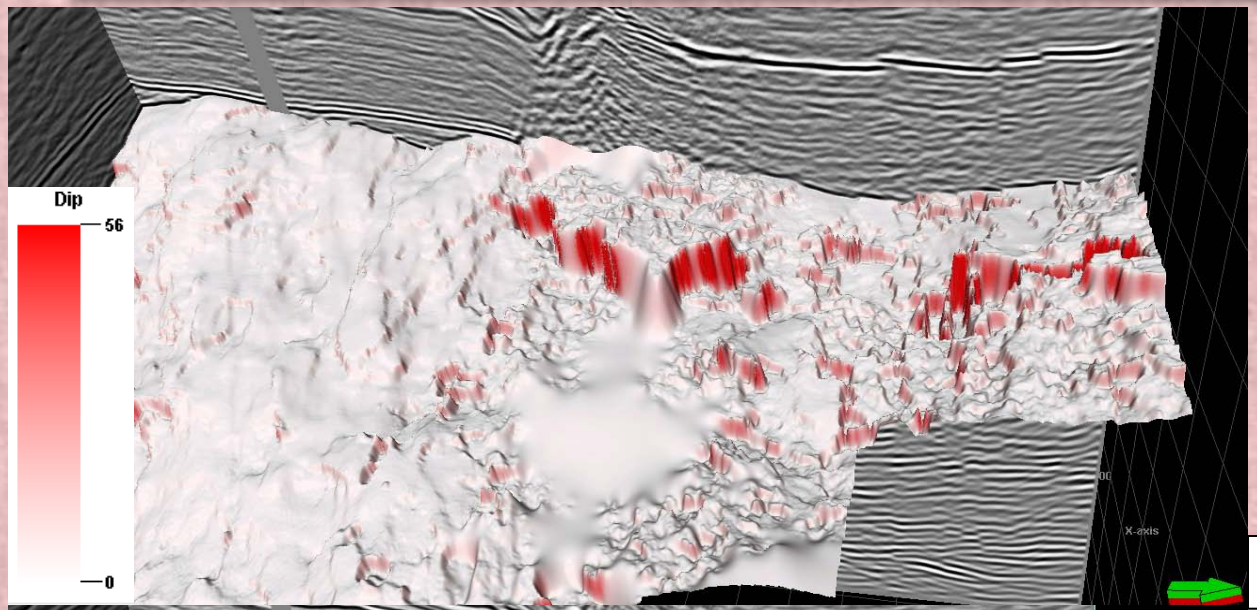

N

Horizon slice of the dip magnitude through the basement surface.

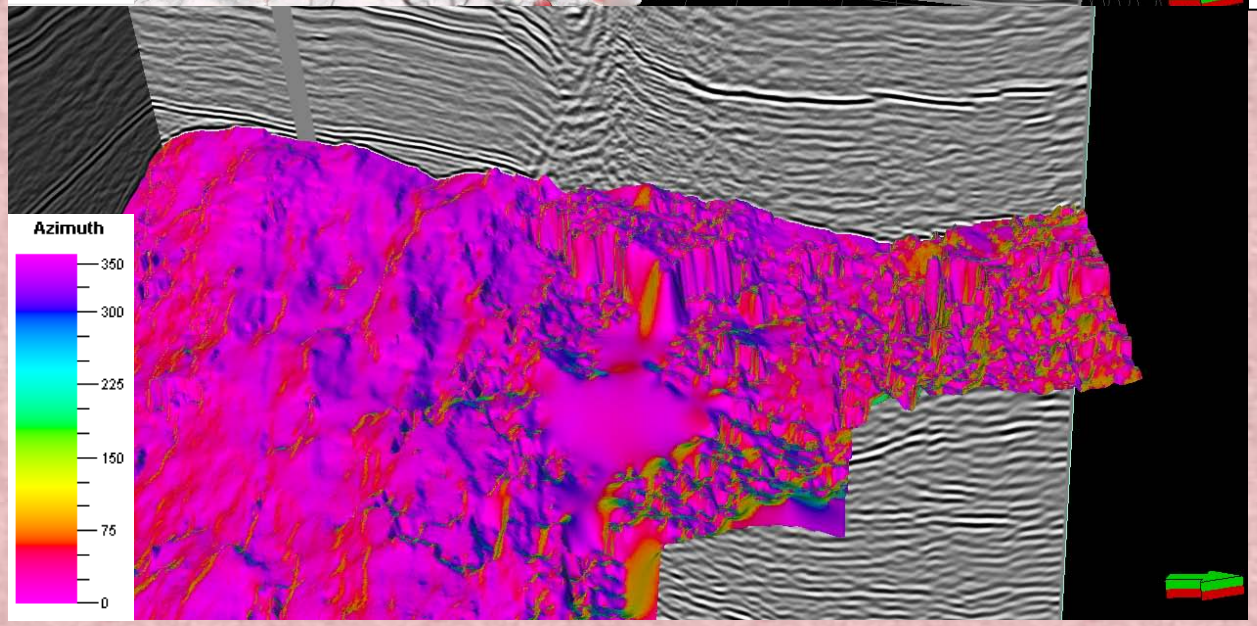

Horizon slice of the dip azimuth shows the general dip (magenta) is towards the north and north east with irregular dips in different directions.

3D Seismic Data and Seismic Attributes

Seismic attributes through the basement Surface

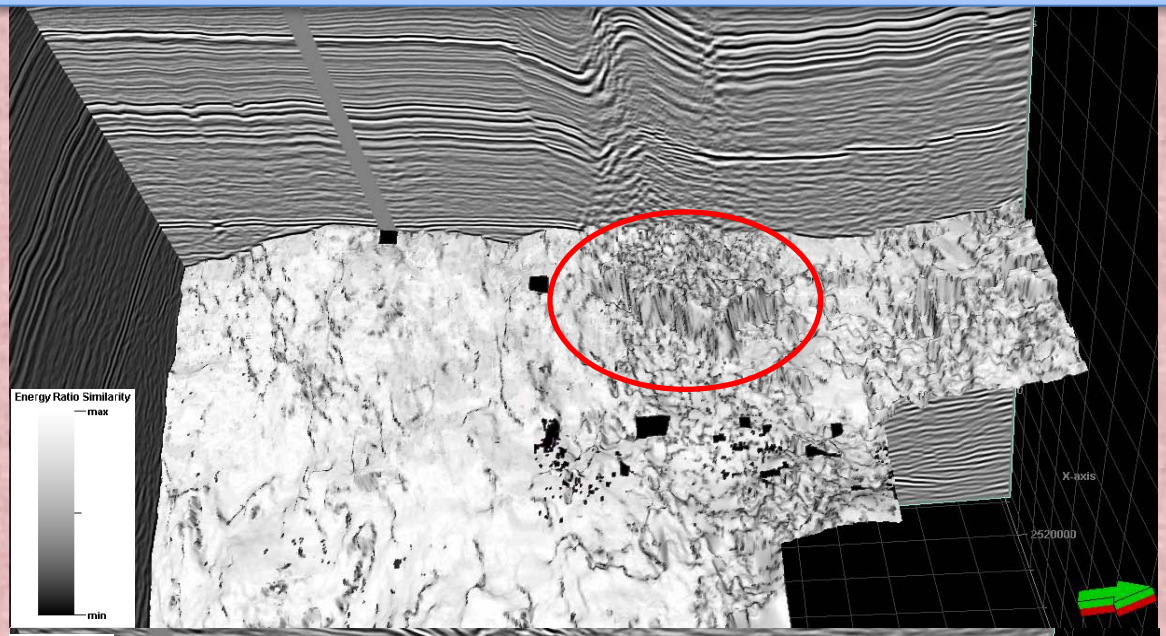

Horizon slice of coherence through the basement surface shows low coherent zone in dark color corresponding to the deformed block.

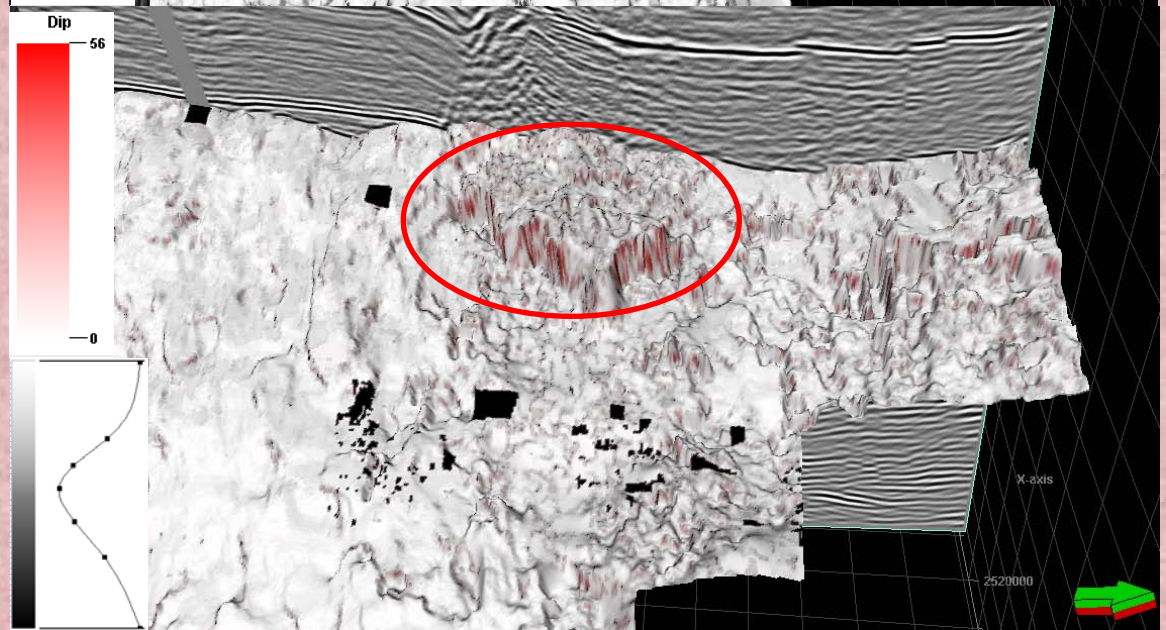

Co-rendered horizon slices of the dip magnitude and the coherence show a good correlation between low coherence and high dip angle deformed zone.

Comparison of Results from Magnetic and Seismic data

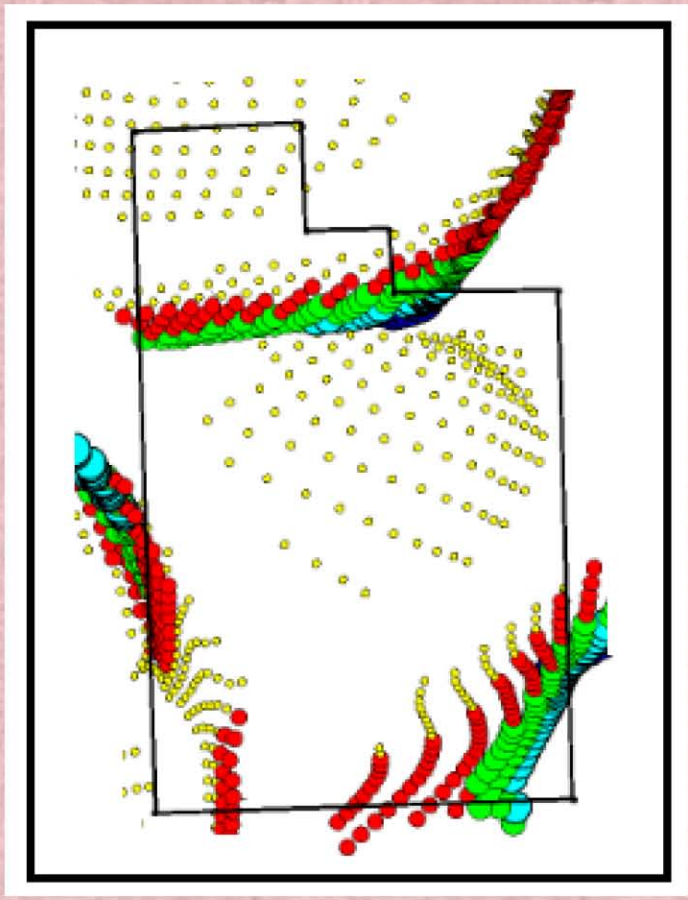

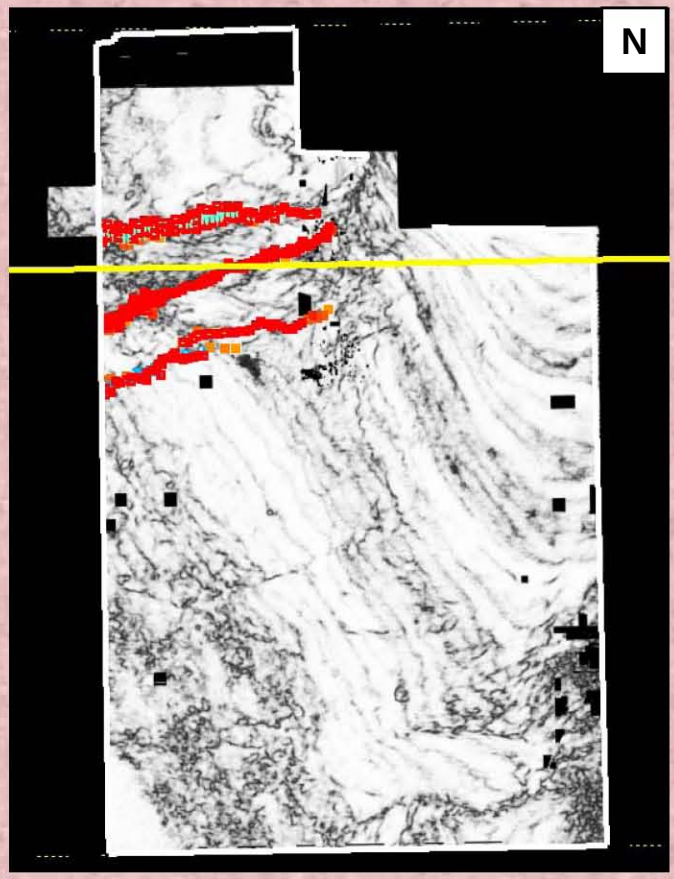

Euler solution cluster plot and time slice (1500 ms) through the coherence volume showing a good correlation of the fault trends.

Modeling
Density models

BASEMENT_WELLS2.gdb

D0:0	Base_Subsea_m	Latitude	Longitude	UTM_X	utm_y	BasementWells
0.0	163	34.26766	-96.47956	732052.20042579	3794709.19073024	
1.0	128	34.20584	-96.47517	732626.59414961	3787862.01431073	
2.0	245	34.34121	-96.44904	734657.94747510	3802937.72897741	
3.0	231	34.34302	-96.44417	735100.98245425	3803149.77513539	
4.0	33	34.22881	-96.43662	736115.14695359	3790498.65804740	
5.0	79	34.16994	-96.41841	737958.39451544	3784010.99938115	
6.0	207	34.30890	-96.37299	741748.13991099	3799532.17998175	
7.0	196	34.27139	-96.35322	743676.29587514	3795418.55564561	
8.0	-3,260	34.51074	-96.34767	743492.65831079	3821982.59550471	
9.0	198	34.27867	-96.34003	744869.82767447	3796257.80307137	
10.0	195	34.25676	-96.30920	747773.03646747	3793902.08665088	
11.0	12	34.26146	-96.30394	748243.69655410	3794436.27798092	
12.0	74	34.19318	-96.29255	749494.20199772	3786889.98705598	
13.0	90	34.19319	-96.28929	749794.66784667	3786899.08709979	
14.0	78	34.18708	-96.28415	750286.52246869	3786233.93732282	
15.0	-1,663	34.24192	-96.27880	750617.12282076	3792330.39999554	
16.0	66	34.17470	-96.23756	754618.60270143	3784976.09406728	
17.0	83	34.18520	-96.23197	755102.35346406	3786154.83543058	
18.0	180	34.20785	-96.22423	755747.41358399	3788686.80753238	
19.0	-2,273	34.24591	-96.21750	756252.24798079	3792925.75020813	
20.0	-3,969	34.97017	-95.51420	818268.27547232	3875288.04653018	

Arbuckle_wells3.gdb

D0:0	Arb_Subsea_m	Thchi	TD	D	Zo	B	Su	Subb_E	El	Latitude	Longitude	UTM_X	UTM_Y
0.0	-645		0	35	11		0	*	0830	253	34.7396098	-95.5845725	812712.91885650	3849482.38923869
1.0	-587		0	13	4		0	*	0832	254	34.6087749	-95.8477416	789063.30970566	3834178.14383071
2.0	-659		0	74	23		0	*	0712	217	34.7856102	-95.8571173	787589.99835550	3853771.12717434
3.0	-543		0	5	2		0	*	01,05	323	34.6624061	-95.8599875	787754.42595439	3840093.39806072
4.0	-524		0	13	4		0	*	0858	262	34.6040598	-95.9037881	783938.09086680	3833495.63092878
5.0	-629		0	31	9		0	*	0761	232	34.6992831	-95.9576022	778682.12869121	3843909.89839924
6.0	-661		0	22	7		0	*	0791	241	34.5409710	-95.9767691	777452.88829433	3826293.08647277
7.0	-720		0	11	3		0	*	0584	178	34.3781851	-96.0980036	766841.26185339	3807907.37056458
8.0	-667		0	193	59		0	*	0615	187	34.1597422	-96.1072383	766681.36461563	3783650.13495611
9.0	-591		0	15	5		0	*	0760	232	34.6890689	-96.1194415	763885.63232692	3842340.00970730
10.0	-682		0	6	2		0	*	0705	215	34.5276993	-96.1216028	764198.81751459	3824432.14390927
11.0	-674		0	18	5		0	*	0584	178	34.2916443	-96.1321520	763971.58516038	3798217.59093560
12.0	-714		0	13	4		0	585	178585	178	34.1862951	-96.1570488	762005.79732554	3786466.49128774
13.0	-719		0	9	3		0	*	0594	181	34.5623779	-96.1666590	759954.06230022	3828162.30180836
14.0	-750		0	21	6		0	*	0553	169	34.2526131	-96.1736869	760267.72168612	3793780.60281182
15.0	-667		0	52	16		0	*	0679	207	34.3793509	-96.2029785	757182.30316476	3807765.32719424
16.0	-602		0	45	14		0	*	0844	257	34.2139071	-96.2137976	756690.50455954	3789384.98133410
17.0	-595		0	17	5		0	*	0889	271	34.7445691	-96.2323855	753366.49678220	3848206.46239345
18.0	-604		0	11	3		0	*	0831	253	34.7889288	-96.2513275	751497.21668756	3853079.96545619
19.0	-587		0	18	5		0	*	0876	267	34.8482474	-96.2676160	749827.13326417	3859619.88467838
20.0	-615	-2,(	**	246	75		0	*	0636	194	34.2419021	-96.2785675	750638.59466889	3792328.98723255
21.0	-653		0	86	26		0	*	0662	202	34.4953201	-96.3009542	747828.13592435	3820385.62543027
22.0	-609		0	88	27		0	*	0784	239	34.7043853	-96.3057026	746772.27105893	3843566.17491219
23.0	-632		0	11	32	2,82	860	*	0712	217	34.6099268	-96.3503174	742960.69903731	3832979.08624657
24.0	-609		0	60	18		0	*	0802	244	34.7371933	-96.3946025	738533.52619216	3846991.01408619

Line/Group

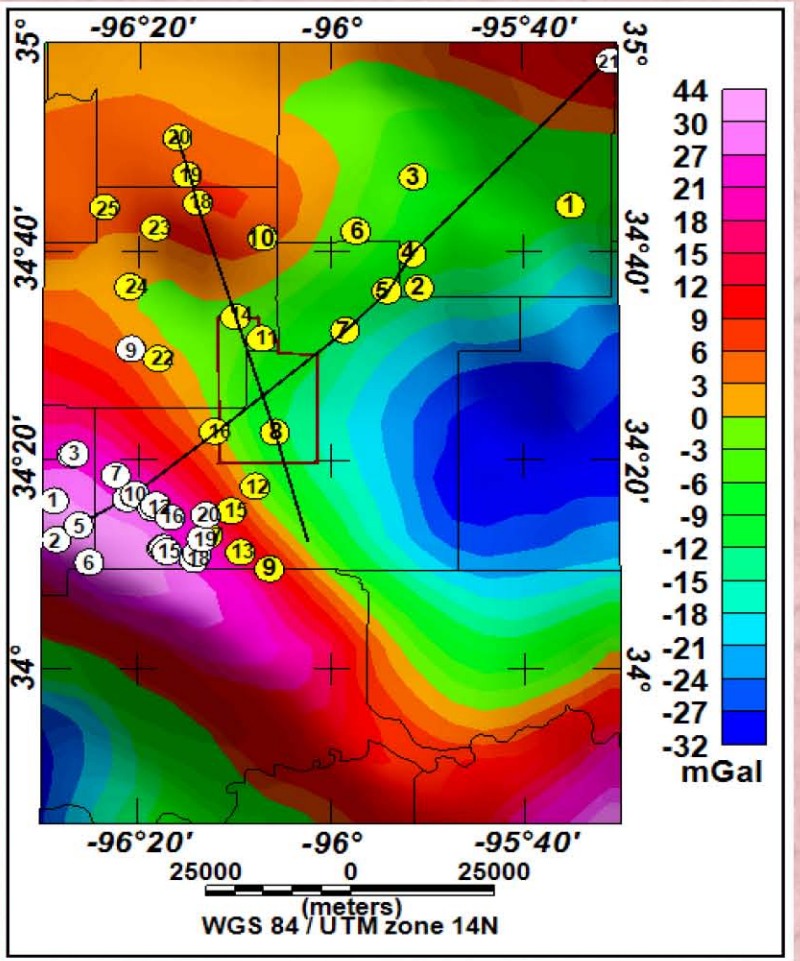

Residual gravity after upward continuation to 40 km shows the location of wells and two selected profiles for the density models.

Regional gravity model

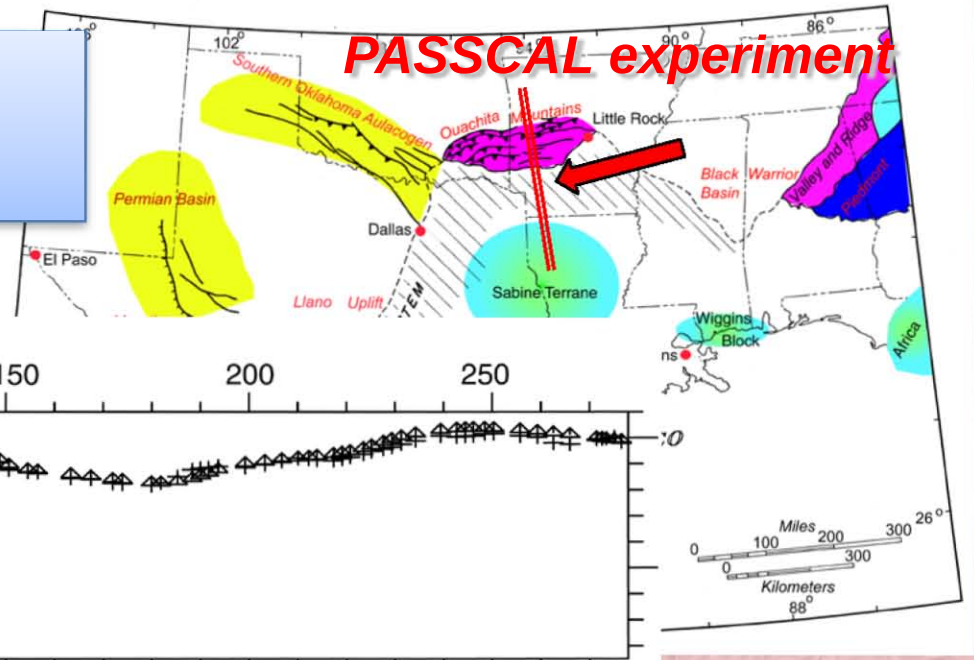

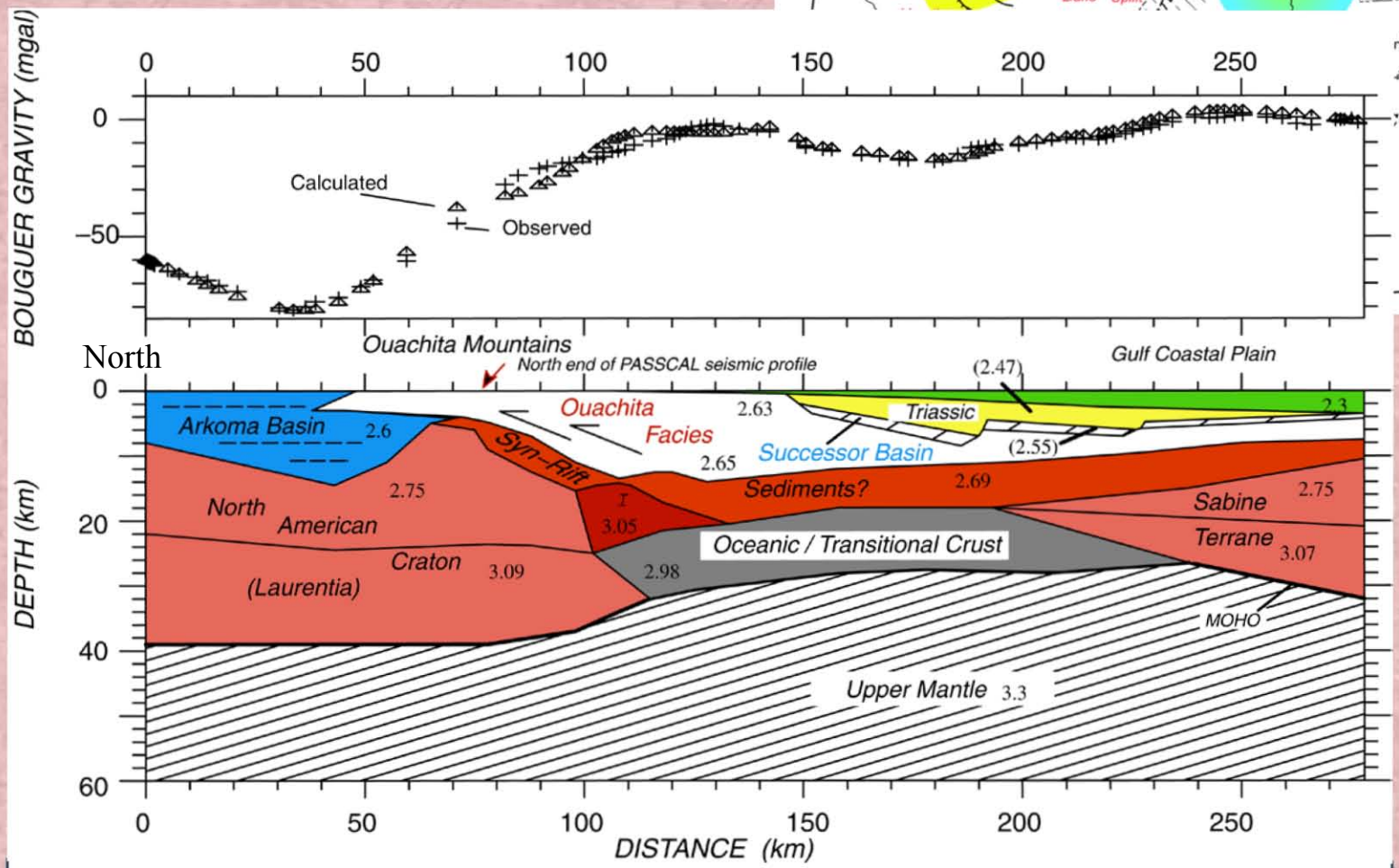

Regional gravity model derived from the PASSCAL Ouachita seismic experiments, COCORP reflection profiles, along with drilling and geological data, (Keller et. Al., 1999)

Density model along NE-SW Profile

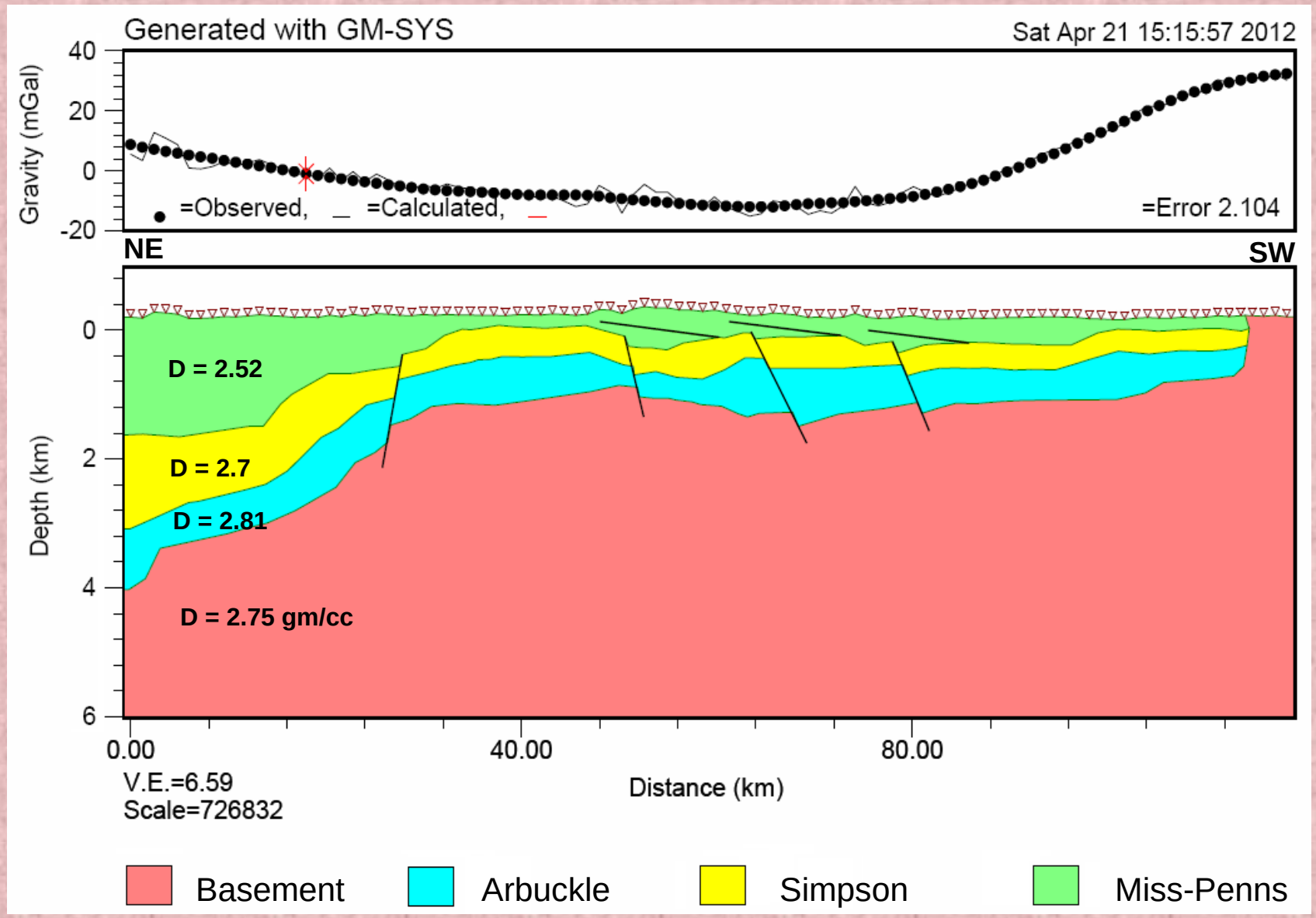

Conclusion

- The basement surface has been subjected to extensive deformation and erosion.
- The maximum depth to the faults which may affect the basement surface is nearly about 3500 meters.
- Seismic and magnetic data show an E-W trend of faulting zone in the northern part of the study area.
- Fault trends from Euler depth estimation method shows very good correlation to the fault trends from seismic data.

Thank you

Cambrian Rifting as Part of the Break-up of Rodinia

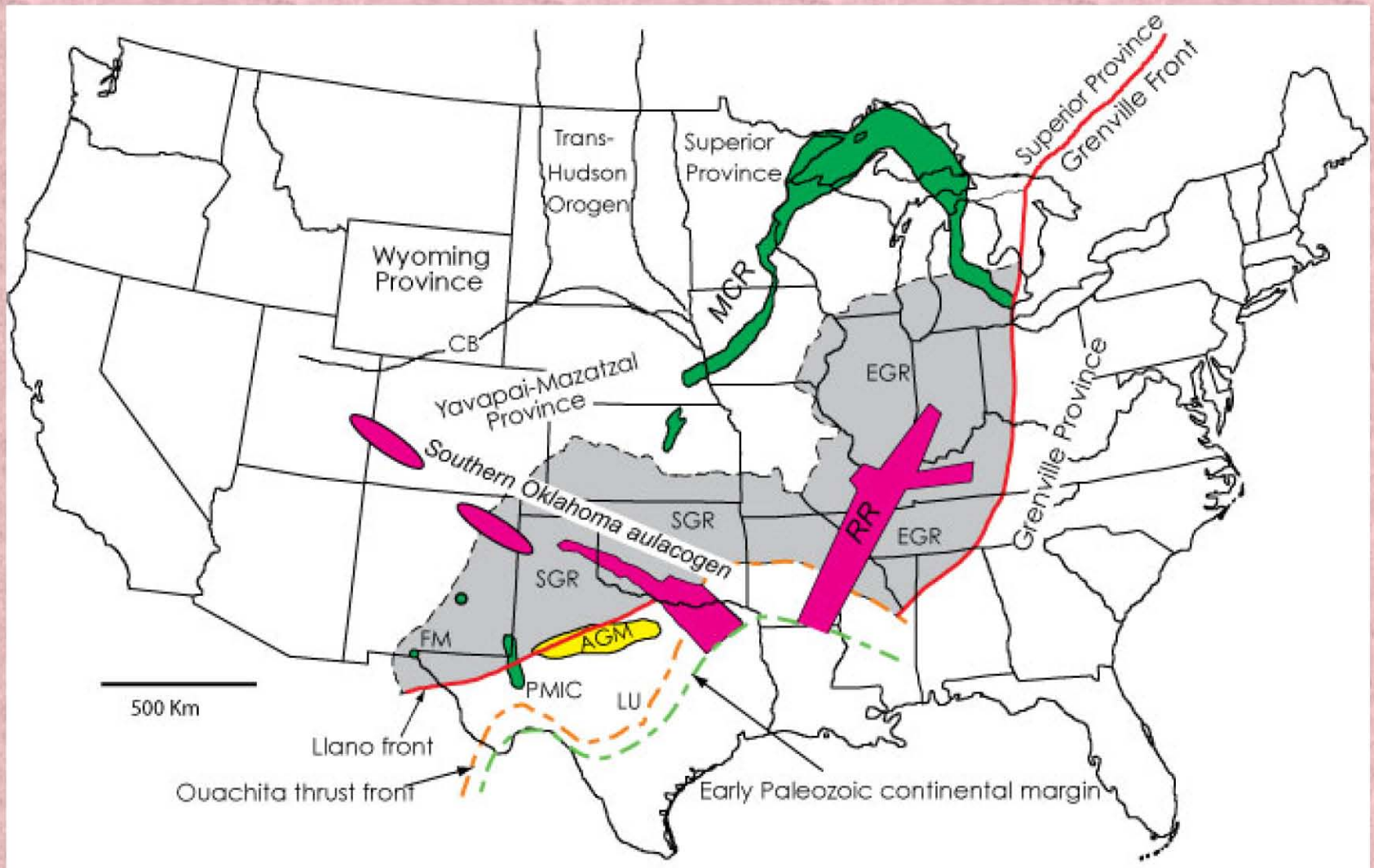

(modified from Barnes and others, 1999, originally modified from Van Schmus and others, 1996).

Edge detection techniques
Tilt Derivative

$$\text{TILT} = \tan^{-1}\frac{\text{vertical component of gradient}}{\text{horizontal component of gradient}}$$

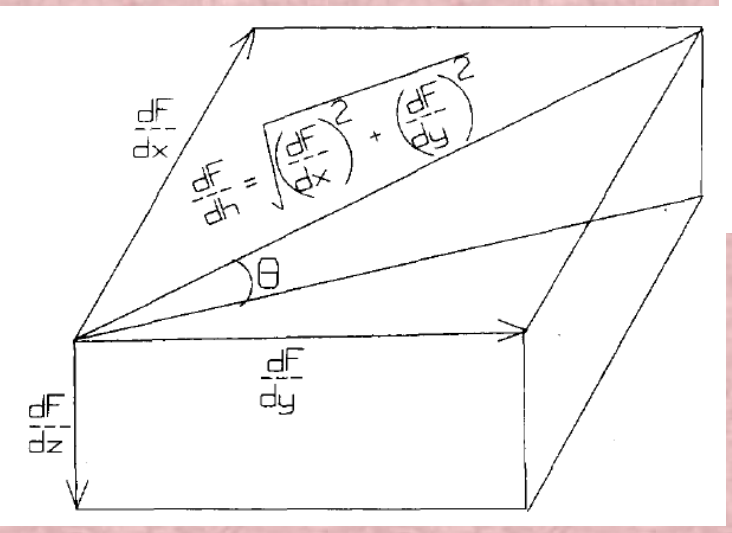

$$= \tan^{-1}\frac{\left(\frac{\partial f}{\partial z}\right)}{\left(\frac{\partial f}{\partial h}\right)}$$

where:

$$\frac{\partial f}{\partial h} = \left[\left(\frac{\partial f}{\partial x}\right)^2 + \left(\frac{\partial f}{\partial y}\right)^2\right]^{1/2}$$

Where, df/dx, df/dy and df/dz are the first-order derivatives in the x, y and z directions

$$(x - x_0)\partial T/\partial x + (y - y_0)\partial T/\partial y + (z - z_0)\partial T/\partial z = A,$$

where A incorporates amplitude, strike, and dip factors

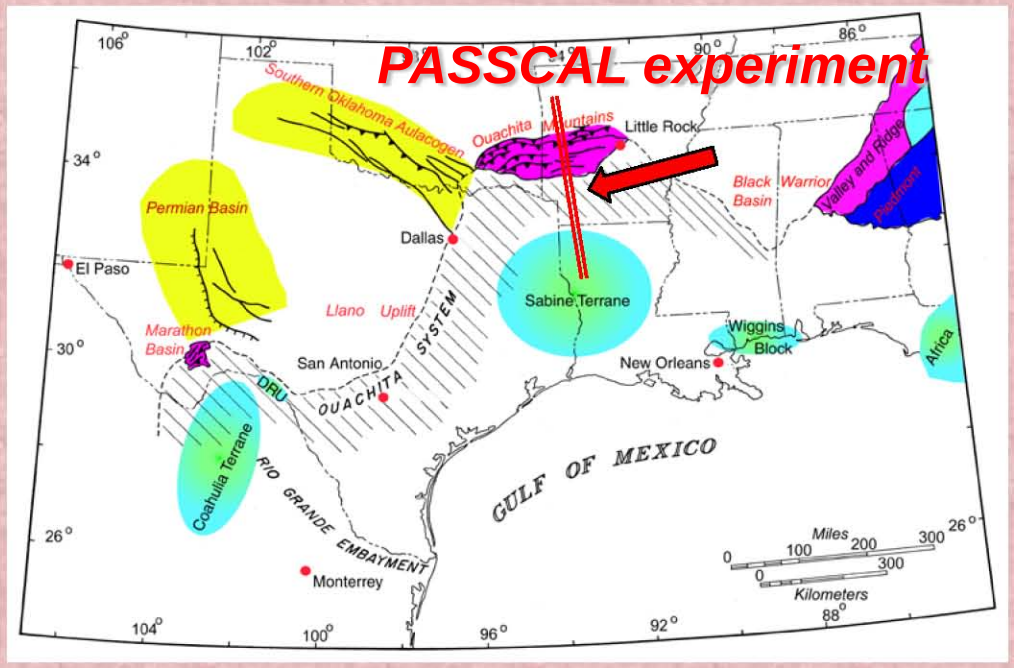

Regional velocity model across the Ouachita mountains. Numbers show velocities in m/sec, Keller et al 1989b & Keller and Hatcher 1999

PASSCAL Experiment Seismic Model

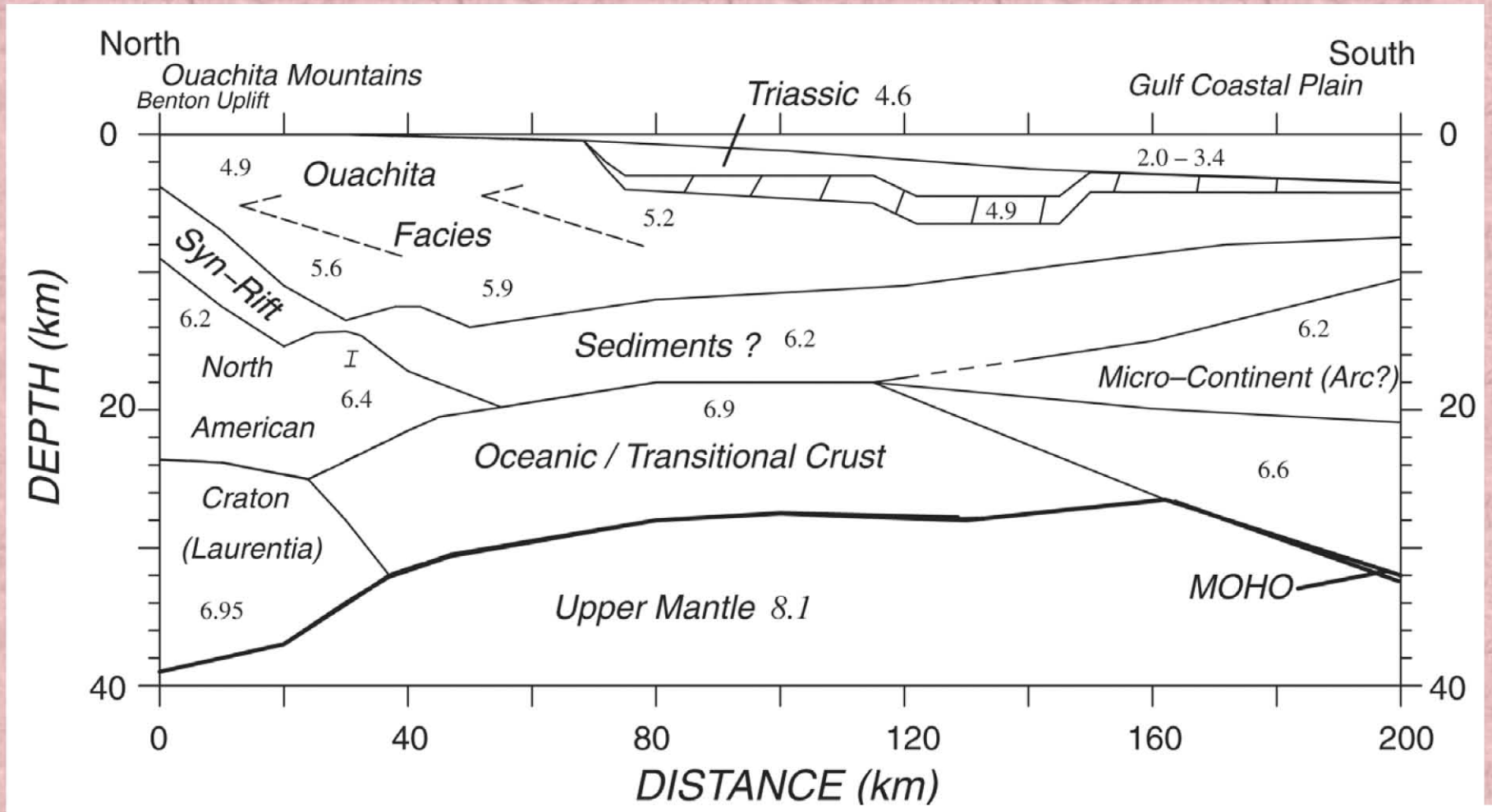

Figure 4. Ouachita PASSCAL seismic experiment velocity model. Modified from Keller et al. (1989b) and Keller and Hatcher (1999). Numbers are velocities in km/s.

A velocity model derived from the PASSCAL Ouachita seismic experiments, COCORP reflection profiles, gravity and magnetic data, along with drilling and geological data in an integrated